Notes on
1.63 Advanced Environmental Fluid Mechanics
Instructor: C. C. Mei, 2002
ccmei@mit.edu, 1 617 253 2994

December 17, 2002

6.7 Thermohaline (double-diffusive) instability in a porous layer

[Refs]: Porous Media:

Cheng, Ping, 1978. Heat Transfer in Geothermal Systems, *Advances in Heat Tranfer*, 14, 1-105.
Nield & Bejan, *Convection in Porous Media* .
O. M. Phillips, 1991 *Flow and Reactions in Permeable Rocks*, Cambridge Univ. P.
Imhoff & Green 1988, Experimental investigation of double diffusive ground water fingers. *J. Fluid Mech.* , 188, 363-382.
R. W. Griffiths, (1981) Layered double-diffusive convection in porous media. *J. Fluid Mech.* 102, 221-248.

Oceanography:

M.E. Stern (1960) The salt fountain and thermohaline convection *Tellus* 12, 172-175.
J. S. Turner, (1973)*Buoyancy Effects in Fluids* Cambriodge.
A. Brandt & H. J. S. Fernando: *Double-diffusive Convection* Geophysics Monograph 94, 1995, AGU.
Raymond Schmitt, 1994. Double diffusion in oceanogrphy, *Annual Rev. Fluid Mech.*255-286.
P. K. Kundu, (1990) *Fluid Mechanics* , Academic.

– – – – – – – – – – – – –

In Salton Sea geothermal field of Imperial Valley, California, the temperature in the hotwater reservoir can be $360°C$. Salinity in groundwater is as high as 2.5×10^5 ppm. Due to sharp contrast of thermal and salt diffusivities ($\kappa_T \sim 1.5 \times 10^{-7} m^2/s, \kappa_S \sim 1.5 \times 10^{-9} m^2/s$), convection can result from instability. This is called thermohaline convection.

In the context of oceanography, this mechanism was first discovered by Melvin Stern (1960).

6.7.1 Heuristic picture

Monotone instability

Consider a fluid lighter at the top and denser at the bottom, with T and C shown in Figure 6.7.1. so that $dT/dz, dC/dz > 0$.

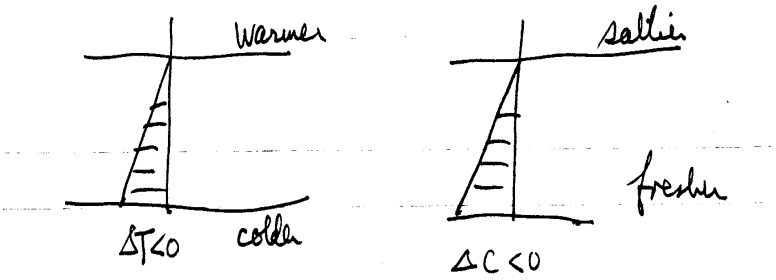

Figure 6.7.1: Salinity and temperature profiles favoring monotonic instability in a porous medium

Let a fluid parcel rise from z to $z + \Delta z$. Because the thermal diffusivity κ_m is much greater than the mass difffusivity of salt, κ_s, the rising water parcel absorbs heat much more quickly than it absorbs salt. Hence, it can becomes lighter than the surrounding fluid and continue to rise. If a fluid parcel drops by Δz, the faster heat loss can make it heavier than its sourounding fluid and sinking continues. Thus the fluid system can be unstable. This instability leads to fingering. See Figure 6.7.2 for the Hele-Shaw model of fingering in a porous medium Imhoff & Green have also given laboratory evidence of fingering as a result of such instability as shown in Figure **??**. The mechanism can be of interest in the transport of contaminants in ground water.

Motivated by oceanographic interest, Turner has performed laboratory experiments shown in Figure 6.7.5 for more rapidly diffusing salt solution on top of denser sucrose solution. Figure 6.7.5 shows the fingering by pouring hot dilute salt solution on top of a stable temperature gradient.

Oscillatory instability Consider a cold and fresh water lying over a warm and salty water. Assume that the the fluid density decreases with height. The profiles of T and C are shown in figure 6.7.6 so that $dT/dz, dC/dz < 0$.

A lighter fluid parcel accidentally moved up by Δz will cool off quickly while losing little salt. Hence, it will come down, resulting in oscillations. However, theory will show later that the noninstantaneous heat transfer leads to unstable growth of the oscillations, resulting in a mixed layer where the salinity and temperature are relatively uniform. At the top of this mixed layer, the salinity is rather discontiuous because of weak diffiusivity. But the temperture profile has a smoother transition because of the large diffusivity. The density profile is contiuous. Now this thermal boundary layer is like a Rayleigh -Benard (or Horton-Rogers-Lapwood) problem. When the jump become large enough The critical Rayleigh number is exceeded so that Benard/Lapwood convection cells appear as sketched in

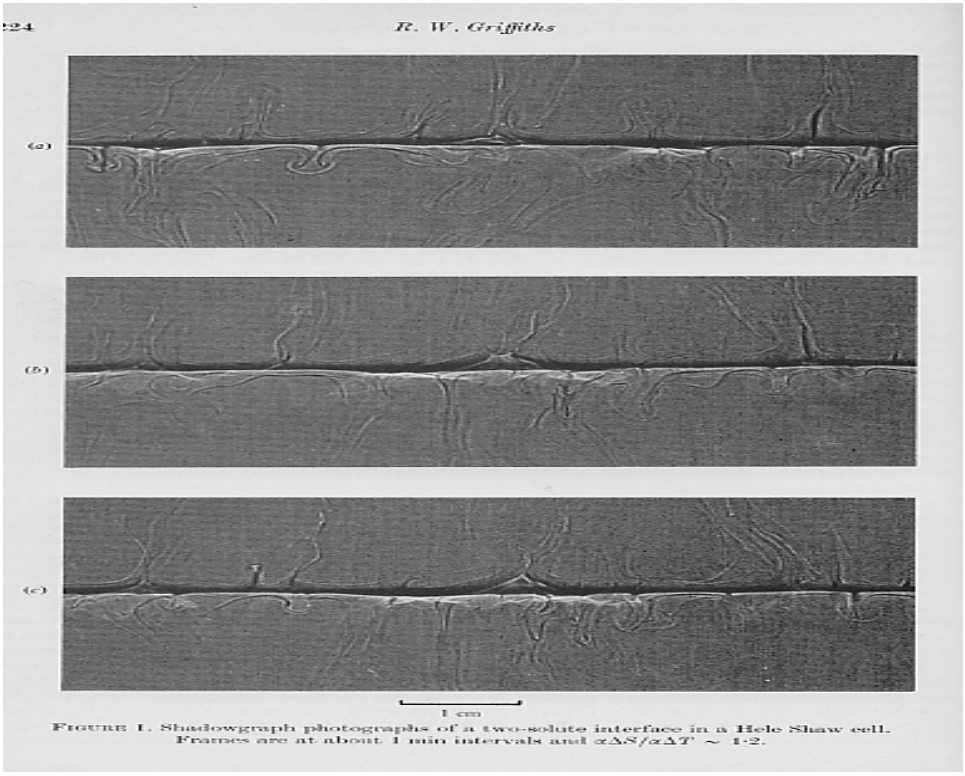

FIGURE 1. Shadowgraph photographs of a two-solute interface in a Hele Shaw cell. Frames are at about 1 min intervals and $\alpha\Delta S/\alpha\Delta T \sim 1{\cdot}2$.

Figure 6.7.2: Development of fingering at the interface of salt/sugar solutions. (Griffiths, 1981)

Figure **??**. This process continues until another mixed layer develops. Eventually a staircase profile is developed, as sketched in figure 6.7.8.

We shall explain the initial instability theory.

6.7.2 Governing equations

Conservation of Fluid Mass:

$$\nabla \cdot \vec{u} = 0 \tag{6.7.1}$$

Conservation of fluuid momentum:

$$0 = -\nabla p - \frac{\mu}{k}\mathbf{u} + \rho_f \vec{g} \tag{6.7.2}$$

Energy:

$$\sigma \frac{\partial T}{\partial t} + \mathbf{u} \cdot \nabla T = \kappa_m \nabla^2 T, \tag{6.7.3}$$

$$\sigma = \frac{(\rho c)_{fluid}}{(\rho c)_{mix}}$$

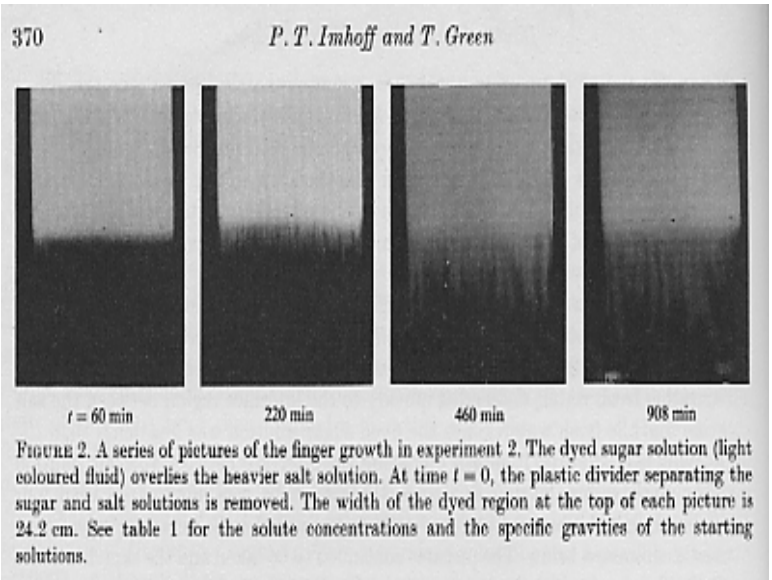

FIGURE 2. A series of pictures of the finger growth in experiment 2. The dyed sugar solution (light coloured fluid) overlies the heavier salt solution. At time $t = 0$, the plastic divider separating the sugar and salt solutions is removed. The width of the dyed region at the top of each picture is 24.2 cm. See table 1 for the solute concentrations and the specific gravities of the starting solutions.

Figure 6.7.3: Fingering at salt/sucrose interface, by Imhopf and Green.

Conservation of Salinity :

$$n\frac{\partial C}{\partial t} + \mathbf{u}\cdot\nabla C = \kappa_s \nabla^2 C \tag{6.7.4}$$

Equation of state:

$$\rho_f = \rho_0\left[1 - \beta\left(T - T_0\right) + \beta_s\left(C - C_0\right)\right] \tag{6.7.5}$$

Note the sign difference of thermal expansion coefficient and salinity.

Static equilibrium:

$$\mathbf{u} = 0 \tag{6.7.6}$$

$$\begin{aligned} T_s &= T_0 + \Delta T\left(1 - \frac{z}{H}\right) \\ C_s &= C_0 + \Delta C\left(1 - \frac{z}{H}\right) \end{aligned} \tag{6.7.7}$$

$$P_S = P_0 - \rho_0 g\left[z - \frac{\beta}{2}\Delta T\left(2z - \frac{z^2}{H}\right) + \frac{\beta_S}{2}\Delta C\left(2z - \frac{z^2}{H}\right)\right] \tag{6.7.8}$$

6.7.3 Perturbed flow

Let $\mathbf{u} = \mathbf{u}'$ be the velocity disturbance, and let

$$T = T_s + T', \qquad p = p_s + p', \qquad C = C_s + C'$$

The perturbations must satisfy:

$$\nabla\cdot\mathbf{u}' = 0 \tag{6.7.9}$$

$$0 = -\nabla p' - \frac{\mu}{k}\mathbf{u}' - \rho_0\left(\beta T' - \beta_s C'\right)\mathbf{g} \tag{6.7.10}$$

$$\sigma\frac{\partial T'}{\partial t} - w'\frac{\Delta T}{H} = \kappa_m \nabla^2 T' \tag{6.7.11}$$

$$n\frac{\partial C'}{\partial t} - w'\frac{\Delta C}{H} = \kappa_s \nabla^2 C' \tag{6.7.12}$$

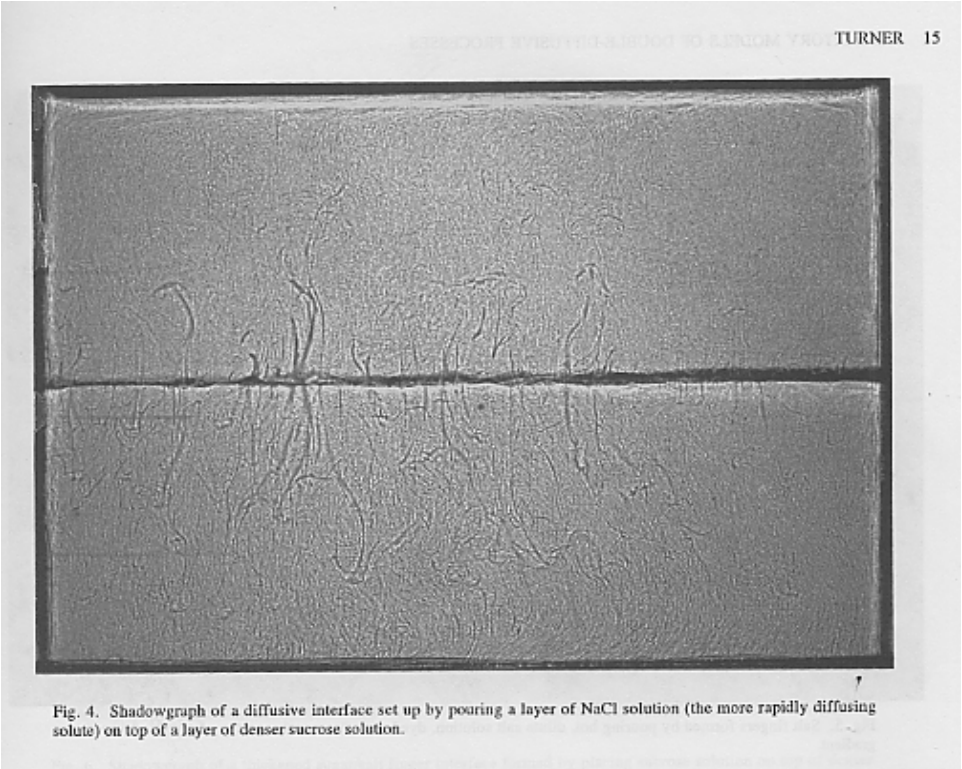

Fig. 4. Shadowgraph of a diffusive interface set up by pouring a layer of NaCl solution (the more rapidly diffusing solute) on top of a layer of denser sucrose solution.

Figure 6.7.4: Fingering along the interface of a salt solution (more diffusive and lighter) on top a sugar solution (less diffusive and heavier). J. S. Turner in *Double Diffusive Convection*, edited by A Brandt an H.J. Fernando, 1995

6.7.4 Normalization

$$\begin{aligned} (x,y,z) &= H(x^*,y^*,z^*), \qquad \nabla = \frac{\nabla^*}{H} \\ t &= \frac{\sigma H^2}{\kappa_m} t^*, \qquad \mathbf{u}' = \frac{\kappa_m}{H}\mathbf{u}^* \qquad T' = |\Delta T| T^* \\ C' &= |\Delta C| C^* \qquad p' = \frac{\mu \kappa_m}{k} p^* \end{aligned} \tag{6.7.13}$$

The dimensionless equations, are, with $*$ omitted for brevity,

$$\nabla \cdot \mathbf{u} = 0 \tag{6.7.14}$$

$$-\nabla p - \mathbf{u} + \left(RaT - \frac{Ra_s}{Le} C \right) \mathbf{e_3} = 0 \tag{6.7.15}$$

$$\frac{\partial T}{\partial t} - w = \nabla^2 T \tag{6.7.16}$$

$$Le \left(n \frac{\partial C}{\partial t} - W \right) = \nabla^2 C, \tag{6.7.17}$$

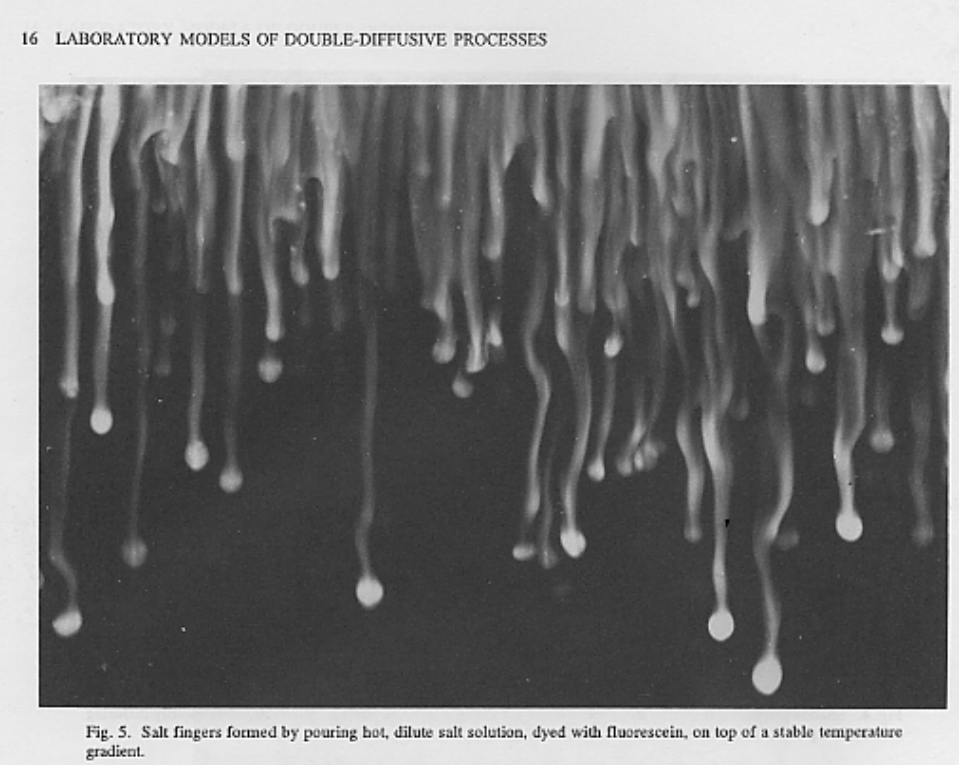

Figure 6.7.5: Fingering due to double-diffusive stability/instability in water. J. S. Turner in *Double Diffusive Convection*, edited by A Brandt an H.J. Fernando, 1995

where

$$Ra = \frac{g\beta k H \Delta T}{\nu \kappa_m} = \text{ thermal Rayleigh No.} \tag{6.7.18}$$

$$Ra_s = \frac{g\beta_s k H \Delta C}{\nu \kappa_s} = \text{salinity Rayleigh No.} \tag{6.7.19}$$

$$Le = \frac{k_m}{k_s} = \text{Lewis No..} \tag{6.7.20}$$

Note that

$$Ra_s = Ra\, N\, Le, \tag{6.7.21}$$

where

$$N = \frac{\beta_s \Delta C}{\beta \Delta T} \tag{6.7.22}$$

can be either positive or negative. Taking curl of Eqn. (6.7.15)

$$\nabla \times \mathbf{u} = Ra \left\{ (T_y - NC_y)\, \mathbf{e_1} - (T_x - NC_x)\, \mathbf{e_2} \right\}. \tag{6.7.23}$$

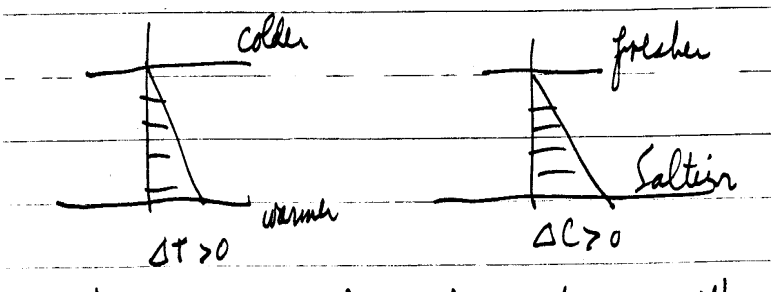

Figure 6.7.6: Salinity and temperature profiles favoring oscillatory instability in a porous medium

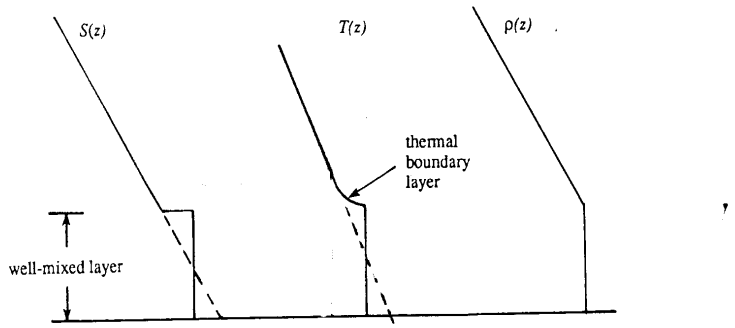

Distributions of salinity, temperature, and density, generated by heating a linear salinity gradient from below.

Figure 6.7.7: From Kundu fig 11.9

Taking curl of the above and using $\nabla \cdot \mathbf{u} = 0$

$$\begin{aligned} \nabla^2 \mathbf{u} &= -Ra \left\{ \left(T_{xz} - NC_{xz} \right) \mathbf{e_1} + \left(T_{yz} - NC_{yz} \right) \mathbf{e_2} \right. && (6.7.24) \\ &\quad \left. - \left[\left(T_{xx} + T_{yy} \right) - N \left(C_{xx} + C_{yy} \right) \right] \mathbf{e_3} \right\} . && (6.7.25) \end{aligned}$$

The z component is

$$\nabla^2 w = Ra \left(\nabla_2^2 T - N \nabla_2^2 C \right) , \qquad \nabla_2 = \frac{\partial^2}{\partial x^2} + \frac{\partial^2}{\partial y^2} \tag{6.7.26}$$

with the boundary conditions,

$$w = T = C = 0, \quad \text{at} \quad z = 0, 1. \tag{6.7.27}$$

Consider sinusoidal disturbances

$$\begin{pmatrix} W \\ T \\ C \end{pmatrix} = \begin{pmatrix} \tilde{W} \\ \tilde{T} \\ \tilde{C} \end{pmatrix} e^{-i\omega t + il x + imy} \tag{6.7.28}$$

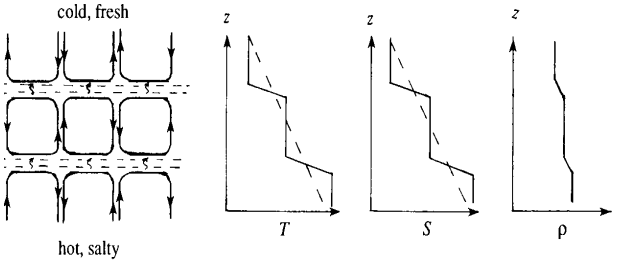

(b) Diffusive regime

ig. 11.7 Two kinds of double-diffusive instabilities. (a) Finger instability, showing up- and lown-going salt fingers and their temperature, salinity, and density. Arrows indicate direction of notion. (b) Oscillating instability, finally resulting in a series of convecting layers separated by diffusive" interfaces. Across these interfaces T and S vary sharply, but heat is transported much aster than salt.

Figure 6.7.8: From Kundu, Fig 11.7b

From Eqn. (6.7.26)

$$\left(D^2 - a^2\right)\tilde{W} = -a^2 Ra\left(\tilde{T} - N\tilde{C}\right) \tag{6.7.29}$$

From Eqn. (6.7.16)

$$-i\omega\tilde{T} - \tilde{W} = \left(D^2 - a^2\right)\tilde{T} \tag{6.7.30}$$

From Eqn. (6.7.17)

$$\left(-i\omega n\tilde{C} - \tilde{W}\right) Le = \left(D^2 - a^2\right)\tilde{C} \tag{6.7.31}$$

where

$$D = \frac{d}{dz} \qquad \text{and} \quad a^2 = \ell^2 + m^2$$

The boundary conditions are

$$\tilde{W} = \tilde{T} = \tilde{C} = 0, \quad z = 0, 1 \tag{6.7.32}$$

Applying the operator

$$\left(D^2 - a^2 + i\omega\right)\left(D^2 - a^2 - i\omega nLe\right)$$

on Eqn. (6.7.29) and using Eqns. (6.7.30) and (6.7.31), we get

$$\begin{aligned}&\left(D^2 - a^2 + i\omega\right)\left(D^2 - a^2 + i\omega nLe\right)\left(D^2 - a^2\right)\tilde{W} \\ &\quad -a^2 Ra\sigma\left(D^2 - a^2 + i\omega nLe\right)\tilde{W} + a^2 Ra_s\left(D^2 - a^2 + i\omega\right)\tilde{W} = 0\end{aligned} \tag{6.7.33}$$

The boundary conditions are

$$\tilde{W} = 0 \tag{6.7.34}$$

$$D^2\tilde{W} = 0 \ \text{ see (6.7.29)} \tag{6.7.35}$$

$$D^4\tilde{W} = 0 \ \text{ see (6.7.30) \& (6.7.31)} \tag{6.7.36}$$

Similarly one can show that $D^{2n}W = 0$ on the boundaries. Assume the solution

$$W = \sin j\pi z \tag{6.7.37}$$

we get from Eqn. (6.7.33) the eigenvalue condition,

$$\begin{aligned} &-\left(j^2\pi^2+\omega^2\right)\left(j^2\pi^2+a^2-i\omega\right)\left(j^2\pi^2+a^2-i\omega nLe\right) \\ &\quad +a^2Ra\sigma\left[j^2\pi^2+a^2-i\omega nLe\right] \\ &\quad -a^2Ra_s\left[j^2\pi^2+a^2-i\omega\right]=0 \end{aligned} \tag{6.7.38}$$

In general ω is complex. At the threshold of instability, $\omega =$ real. From the the real part of (6.7.38):

$$\sigma Ra - Ra_s = \frac{(j^2\pi^2+a^2)}{a^2} - \frac{nLe}{a^2}\omega^2 \tag{6.7.39}$$

From the imaginary part of Eqn. (6.7.38):

$$\omega\left[nLe(\sigma Ra) - Ra_s\right] = \omega\left[\frac{(j^2\pi^2+a^2)}{a^2}(1+nLe)\right] \tag{6.7.40}$$

Both these equations respresent instability thresholds and must hold for real ω.

6.7.5 Monotonic instability

There is no oscillation and the real part of ω is also zero. It follows from (6.7.39) that

$$\sigma Ra - Ra_s = \frac{\left(j^2\pi^2+a^2\right)^2}{a^2} \tag{6.7.41}$$

When there is no salinity, $\Delta C = 0$ and only temperature variation in the background, it is necessary that $\Delta T > 0$ (or $\sigma Ra > 0$, warmer water is at the bottom) for instability. Similarly, when there is no temperature variation ($\Delta T = 0$) and only salinity variation, $\Delta C < 0$ (or $Ra_s < 0$) is necessary for instability. With both effects present, we expect that $\sigma Ra - Ra_s > 0$ corresponds to instability. In particular to find the lowest threshold of instability as a function of a, we take $j = 1$, we take

$$\frac{\partial}{\partial a^2}(\sigma Ra - Ra_s) = 0 \qquad \rightarrow a^2 = \pi^2 \tag{6.7.42}$$

Therefore, the lowest threshold for $\omega = 0$ gives

$$\boxed{\sigma Ra - Ra_s = 4\pi^2} \tag{6.7.43}$$

which is a straight line in Figure 6.7.9. The region of instabilty but lie to the right of this line.

In a Hele-Shaw experiments Griffiths (1981) showed how the fingers evolve after a long time, see Figure 6.7.10

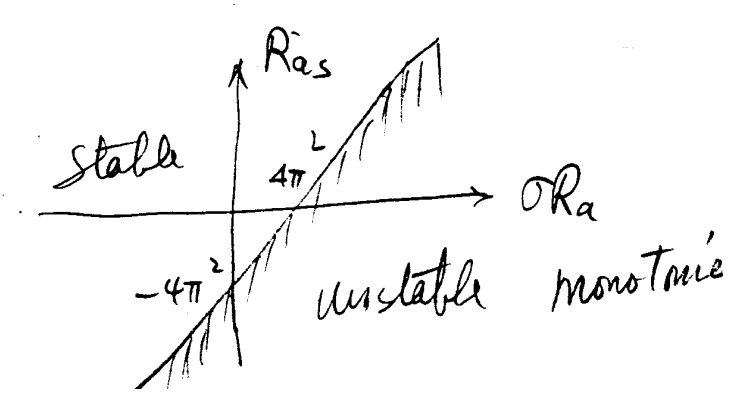

Figure 6.7.9: Domains of montonic stability and instability

6.7.6 Oscillatory instability

We now assume that the real part of $\omega \neq 0$. From Eqn. (6.7.40)

$$nLe(\sigma Ra) - Ra_s = \frac{\left(j^2\pi^2 + a^2\right)^2}{a^2}(1 + nLe)$$

The lowest threshold of oscillatory instability is at : $j = 1, a^2 = \pi^2$

$$\boxed{nLe(\sigma Ra) - Ra_s = 4\pi^2(1 + nLe)} \quad (B) \tag{6.7.44}$$

If $nLe(\sigma Ra) - Ra_s > 4\pi^2(1+nLe)$, oscillatory instability occurs. The frequency of oscillation ω is given by Eqn. (6.7.39)

$$\frac{nLe\omega^2}{\pi^2} = 4\pi^2 - (\sigma Ra - Ra_s) \tag{6.7.45}$$

Since ω is real, we have on the one hand,

$$\boxed{4\pi^2 \geq \sigma Ra - Ra_s}, \quad (A) \tag{6.7.46}$$

for instability. The equality sign is one boundary.

The second boundary is defined by Eqn. (6.7.44) which is a straight line that intersects with Eqn. (6.7.46) at

$$\left(\sigma Ra\right)_c = 4\pi^2 \frac{nLe}{nLe - 1} \quad \text{and} \quad \left(Ra_s\right)_c = \frac{4\pi^2}{nLe - 1}. \tag{6.7.47}$$

Example: $nLe = 2(> 1)$

$$\left(\sigma Ra\right)_c = 8\pi^2, \qquad \left(Ra_s\right)_c = 4\pi^2$$

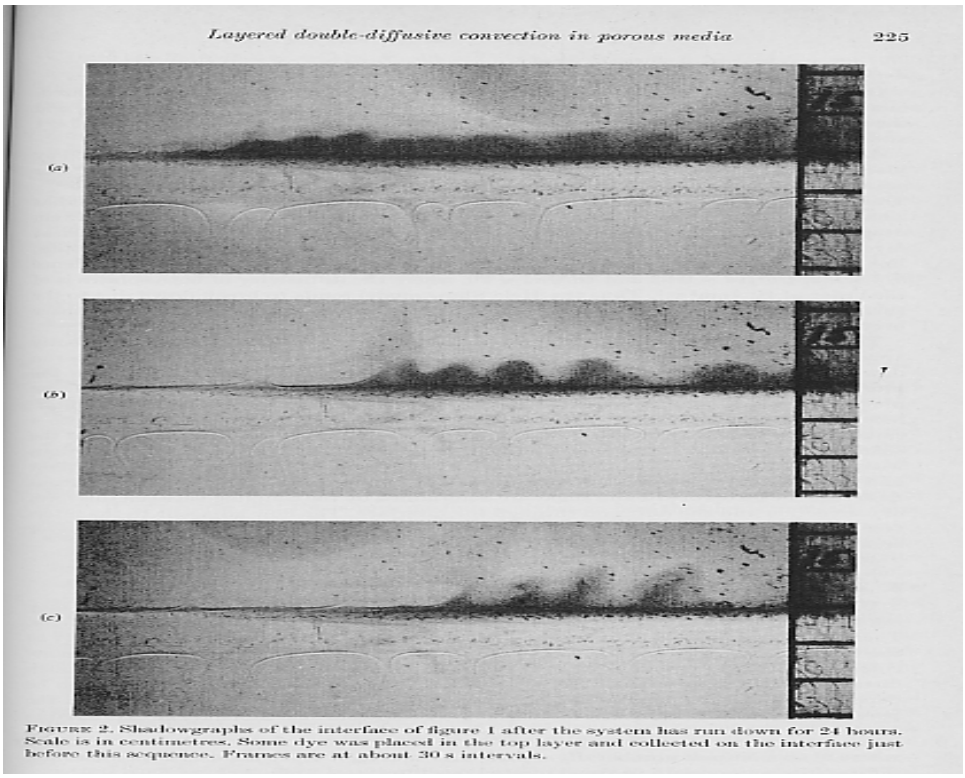

Figure 6.7.10: Development long after fingering at the interface of salt/sugar solutions. (Griffiths, 1981)

Hence the wedge-like region (doubly hatched) of oscillatory instability is in the first quadrant of Figure 6.7.11.

Example: $nLe = 1/2(< 1)$
The second boundary intersects with the first at

$$(\sigma Ra)_c = -4\pi^2 \qquad (Ra_s)_c = -2\left(4\pi^2\right)$$

In this case the wedge-like region (doubly hatched) of oscillatory instability is in the third quadrant of Figure 6.7.12.

– – – – – – – – – – – – – – – – –

Fingering induced by double-diffusive instabilty occurs in oceans where there are strong gradients of temperature and salinity. It has been observed and recorded in Mediteranian Sea "below the warm salty Mediteranian outflow in the eastern North Altlantic and in the western tropical North Altlantc" (Schmitt, 1994). This is reflected by the staircase structure of temperature and salinity profiles, see Figure 6.7.13.

An additional laboratory demonstrations by J.S. Turner is shown in Figure 6.7.14.

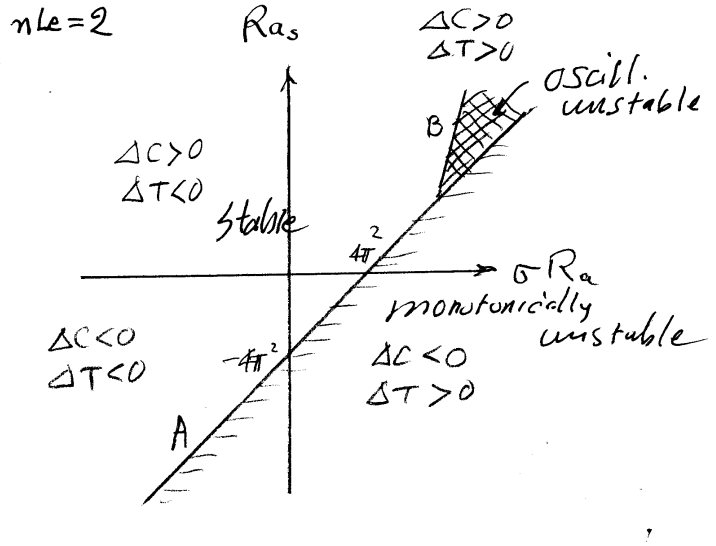

Figure 6.7.11: Domains of stability/instability for $nLe = 2$.

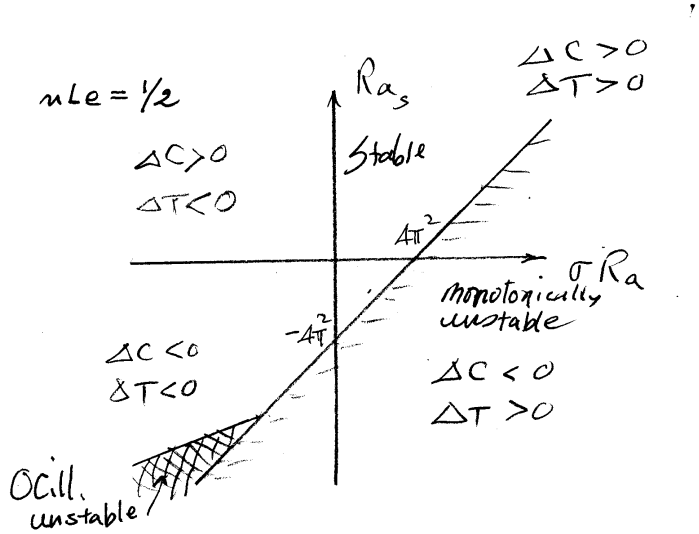

Figure 6.7.12: Domains of stability/instability for $nLe = 1/2$.

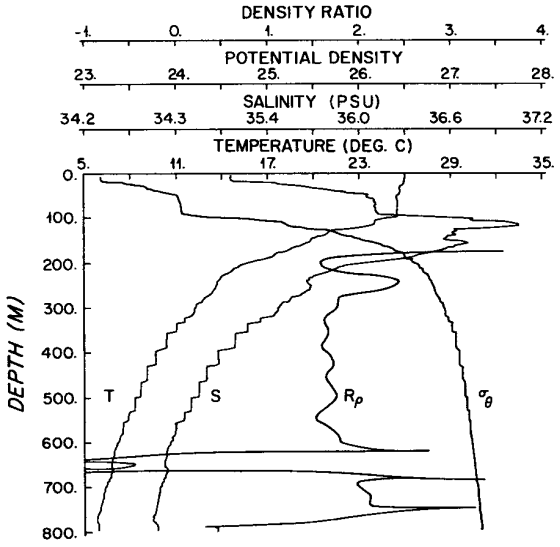

Figure 2 (*b*) The vertical profiles of temperature, salinity, potential density anomaly (σ_θ, kg/m^3), and R_ρ from a station in the C-SALT area, from the surface to 800 m depth. Temperature contrasts across the steps are typically 0.5–1.0°C. Mixed layers are 5–30 m thick. The layered structure in the 300–600 m depth range has $1.5 < R_\rho < 1.8$.

Figure 6.7.13: Vertical profiles in sea water near Barbados, showing thermohaline staircasses (Schmitt, 1994)

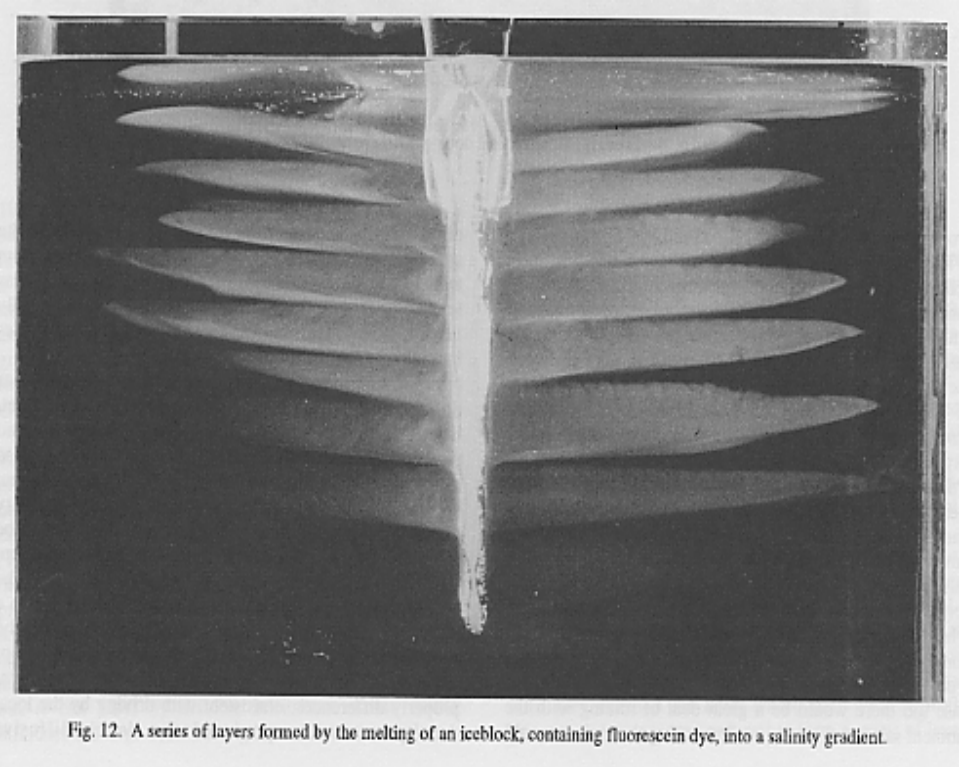

Fig. 12. A series of layers formed by the melting of an iceblock, containing fluorescein dye, into a salinity gradient.

Figure 6.7.14: Fingering near a melting ice in a salt-stratified water. J. S. Turner in *Double Diffusive Convection*, edited by A Brandt an H.J. Fernando, 1995